nature genetics

Dual feedback loops in the *GAL* regulon suppress cellular heterogeneity in yeast

Stephen A Ramsey, Jennifer J Smith, David Orrell, Marcello Marelli, Timothy W Petersen, Pedro de Atauri, Hamid Bolouri & John D Aitchison

Transcriptional noise is known to be an important cause of cellular heterogeneity and phenotypic variation. The extent to which molecular interaction networks may have evolved to either filter or exploit transcriptional noise is a much debated question. The yeast genetic network regulating galactose metabolism involves two proteins, Gal3p and Gal80p, that feed back positively and negatively, respectively, on *GAL* gene expression. Using kinetic modeling and experimental validation, we demonstrate that these feedback interactions together are important for (i) controlling the cell-to-cell variability of *GAL* gene expression and (ii) ensuring that cells rapidly switch to an induced state for galactose uptake.

Transcriptional activation is an intrinsically stochastic process that can leave a signature of cell-to-cell or temporal variation in the activity of a gene[1–5]. On a multigene scale, transcriptional networks frequently possess negative feedback, which can suppress transcriptional noise[6,7], and positive feedback, which can amplify it[8,9].

The *GAL* network in the yeast *Saccharomyces cerevisiae* (**Fig. 1a**) controls galactose transport and metabolism[10–12] and contains both positive and negative feedback[13,14]. Through a single Gal4p binding site in the promoter, *GAL3* and *GAL80* are upregulated in response to galactose, leading to 'dual feedback' on *GAL* expression: positive feedback by Gal3p and negative feedback by Gal80p.

The galactose network response depends on a balance between *GAL3*- and *GAL80*-mediated feedback; disabling the regulation of either gene alone substantially changes the steady-state[13,14] and dynamic[15] response of the system to galactose. Most previous studies of the *GAL* network have focused on the steady-state response[16,17] and did not model the stochastic dynamics of *GAL* induction[13,15].

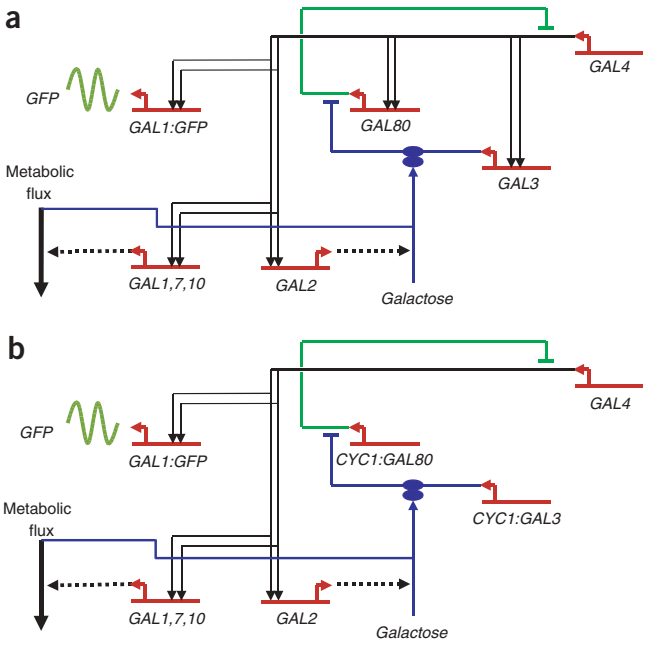

Figure 1 Schematic of the *GAL* network. (**a**) Wild-type strain. (**b**) Mutant strain. The constitutively expressed transcription activator Gal4p binds to the promoters of *GAL* genes. In the absence of galactose, the repressor Gal80p blocks the activation domain of Gal4p (ref. 30). In the presence of intracellular galactose, the signal transducer Gal3p is activated, which sequesters Gal80p in the cytoplasm, leading to transcription of the *GAL* genes[11]. The signal transducer *GAL3* and the repressor *GAL80* are basally expressed in noninduced, non–glucose-repressed conditions. Lines terminating in arrowheads denote positive regulation. Lines terminating in bars denote repression. Gene symbols denote transcription. Dotted lines denote enzymatic interactions. The double ellipses denote galactose activation of Gal3p. The wavy line denotes GFP. The label *GAL1:GFP* denotes the reporter gene, which has a *GAL1* promoter and codes for GFP. 'Metabolic flux' and the thick arrow denote the flux through the Leloir pathway[10], including transformation of galactose into galactose-1-phosphate. Galactose import into the cell is shown by the line originating from 'Galactose'. The very weak *GAL*-activating function of Gal1p (ref. 12) is not shown. In the mutant (**b**), the labels *CYC1:GAL80* and *CYC1:GAL3* denote the genes in which the *CYC1* promoter has been substituted in place of the wild-type *GAL80* and *GAL3* promoters. The absence of black arrows terminating on *CYC1:GAL80* and *CYC1:GAL3* indicates that the regulation of expression of these genes in response to galactose has been disabled.

Institute for Systems Biology, 1441 N 34th Street, Seattle, Washington 98103, USA. Correspondence should be addressed to H.B. (hbolouri@systemsbiology.org) or J.D.A. (jaitchison@systemsbiology.org).

Received 24 January; accepted 28 July; published online 27 August 2006; doi:10.1038/ng1869

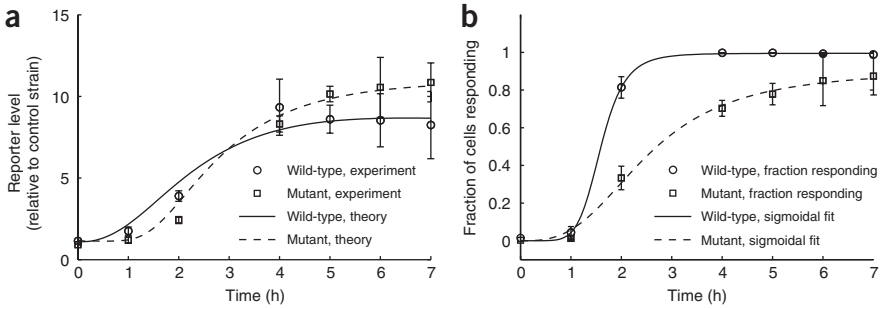

Figure 2 Reporter response to galactose induction. (**a**) Time course of cell population–average fluorescence for cells switched from 2% raffinose to 0.1% galactose (obtained by flow cytometry). Fluorescence is computed relative to the control strain (no GFP). Error bars represent s.d. of four replicate experiments. The theory curves are solutions of the model as a set of ordinary differential equations, using the software program Dizzy[27] with 0.1% external galactose and with initial conditions from the uninduced steady state. The initial Gal80p concentration in the mutant strain was set to twice the wild-type value to account for the induction delay in the mutant strain. A single global scale factor (obtained as described in Methods) was used to convert the simulation results to equivalent fluorescence intensity. During hours 5–7, the mutant induction is an average 24% ± 7% greater than the wild-type. The existence of a delay in the mutant response is consistent with previous theoretical predictions[15]. (**b**) Time course of the fraction of responding cells versus time on 0.1% galactose. A responding cell is defined as having a fluorescence that is greater than three times the control strain. The curves represent a best-fit sigmoidal function (**Supplementary Note**).

We simulated and measured experimentally the time courses of the reporter responses in cells switched from noninducing medium (raffinose) to galactose (**Fig. 2**). The mutant response was initially delayed by ~1 h relative to wild-type, suggesting that feedback is important for a rapid response[18]. After the initial delay, the induction response in the mutant accelerated, overtaking the wild-type response during hours 3–5. By 5–6 h, the responses of both strains approached a steady state.

The fluorescence histograms from the time-course experiment (**Fig. 3**) demonstrate a transiently bimodal distribution of the response in the double-loop-knockout and a uniform rate of response in wild-type cells. By 4–5 h, the mutant population segregated into two groups: those responding and those that did not, whereas the wild-type distribution remained unimodal. The wild-type responded rapidly, with ~80% of the cells responding within 2 h (in contrast to the mutant, with ~30% responding) (**Fig. 2b**). We estimated the time scales for half of the cells to respond as 1.60 h for the wild-type and 2.72 h for the mutant (**Supplementary Note**).

Both experimentally and using a kinetic model, we investigated a perturbation of the *GAL* network in which feedback on *GAL3* and *GAL80* expression is disabled (**Fig. 1b**). Disabling both the *GAL80* and *GAL3* feedback loops results in increased heterogeneity of *GAL* gene expression at a steady state and in a delayed initial cellular response to galactose. These findings suggest an important combined functional role for the *GAL3* and *GAL80* feedback loops in controlling galactose use.

To experimentally test the predictions of our kinetic model (**Supplementary Note**), we generated a double-loop knockout strain in which we placed *GAL3* and *GAL80* under control of the minimal *CYC1* promoter and placed a green fluorescent protein (GFP) reporter under the control of the *GAL1* promoter. The expression levels of *CYC1*-driven *GAL3* and *GAL80* did not increase in response to galactose (**Supplementary Figure 1**). We measured *GAL1* expression in this and the otherwise wild-type strain using flow cytometry.

To understand the reason for the transient bimodal distribution of loop-disabled cells, we solved the kinetic model with respect to the intracellular galactose concentration. The model predicts that the initial rate of galactose uptake is inversely related to the level of Gal80p but insensitive to the level of Gal3p (**Supplementary Fig. 2**). Thus, one possible trivial explanation for the difference between mutant and wild-type responses could be a different average level of Gal80p. However, this is unlikely, because the wild-type has a higher level of Gal80p than the mutant on raffinose (**Supplementary Fig. 1**).

Stochastic simulations showed that, in the uninduced state, the mutant had ~50% greater cell-to-cell variability in Gal80p concentration than the wild-type (**Supplementary Fig. 3**). Cells that reside on the high end of the distribution of Gal80p abundance are delayed

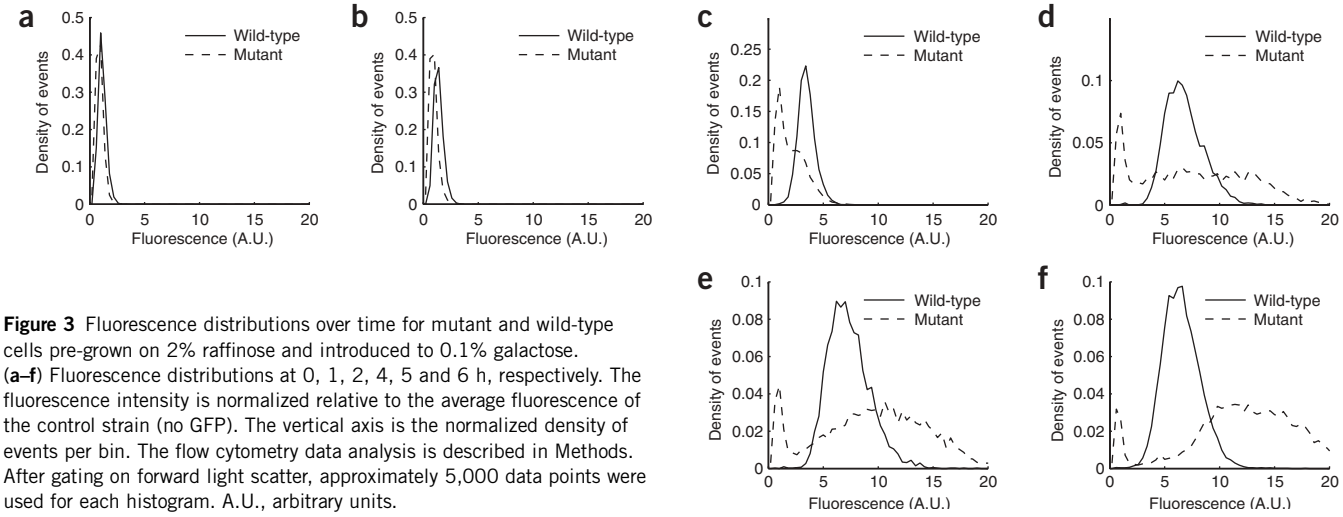

Figure 3 Fluorescence distributions over time for mutant and wild-type cells pre-grown on 2% raffinose and introduced to 0.1% galactose. (**a–f**) Fluorescence distributions at 0, 1, 2, 4, 5 and 6 h, respectively. The fluorescence intensity is normalized relative to the average fluorescence of the control strain (no GFP). The vertical axis is the normalized density of events per bin. The flow cytometry data analysis is described in Methods. After gating on forward light scatter, approximately 5,000 data points were used for each histogram. A.U., arbitrary units.

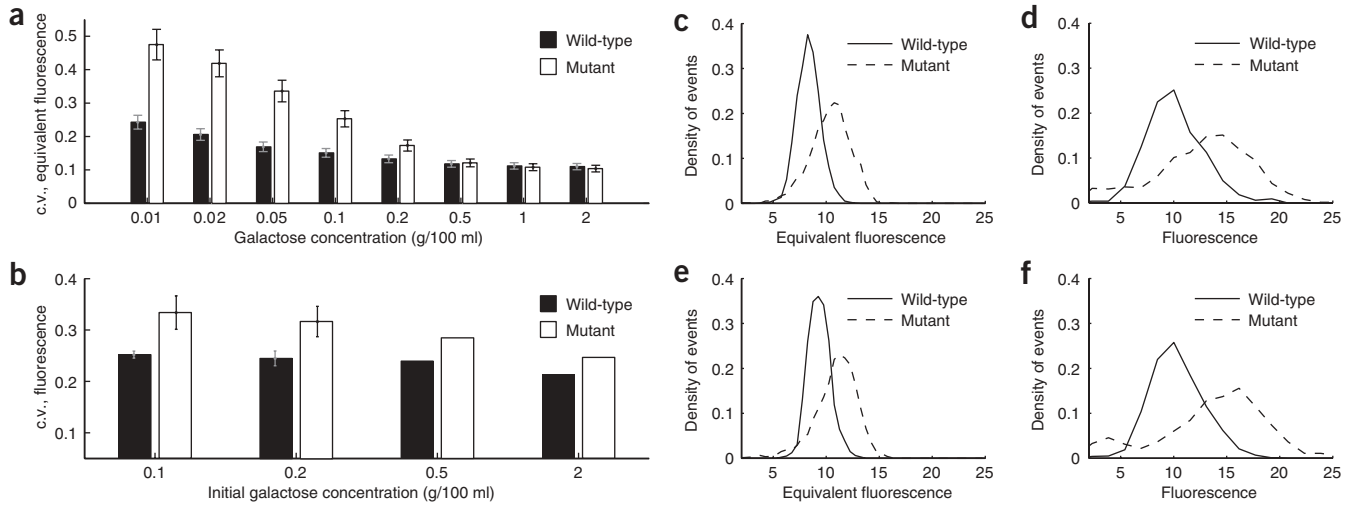

Figure 4 Population heterogeneity of reporter expression. (**a**) Experimentally measured c.v. of fluorescence intensity (relative to the control) for responding cells, as a function of galactose concentration. Error bars represent s.d. for four replicates. (**b**) Predicted c.v. from stochastic simulations of the kinetic model in steady-state conditions at the indicated galactose concentrations. Simulation results were scaled into equivalent fluorescence using the global scale factor obtained from the time-course data (see Methods). In the experimental data, the average (across all four concentrations) ratio of the mutant to the wild-type c.v. is 1.28 ± 0.06; in the model, the average ratio is 1.24. (**c**) Stochastic simulation of an ensemble of 4,800 cells and (**d**) experimentally measured fluorescence intensity at 6 h, for cells grown in 0.1% initial galactose. The width of the distribution of induced cells indicates the variability of *GAL* gene expression. The theory and experiment results for 0.2% galactose are shown in **e** and **f**, respectively. Only responding cells (see Methods) are shown. Both histograms show a normalized density of events after gating based on forward light scatter (approximately 8,200 events per histogram). The experimentally measured ratio of the mutant c.v. to wild-type c.v. is 1.33 for 0.1% galactose and 1.29 for 0.2% galactose. The corresponding ratios from stochastic simulations are 1.68 and 1.30, respectively. The experimental data are overall more variable (which does not affect the ratio of the mutant c.v. to the wild-type c.v., the principal measurement here) owing to additional sources of variability, such as growth rate[5].

in the initial response to galactose, whereas cells at the low end respond rapidly. Simulations also predict that once the mutant cells begin to import galactose, they do so at a higher rate than wild-type (**Supplementary Fig. 2**). Consequently, the expression response of the mutant is able to catch up to the wild-type, and experimentally we observed few mutant cells at intermediate response levels.

Our simulations further predict that, even at a steady state, the mutant population will have greater heterogeneity in its *GAL* gene expression than the wild-type population. Specifically, the coefficient of variation (c.v.) of the reporter level, for cells at steady-state grown on 0.1% galactose (wt/vol), is predicted to be 70% greater in the mutant than in wild-type (**Fig. 4a**). The ratio (mutant c.v. versus wild-type c.v.) is furthermore predicted to decrease with increasing galactose concentration, with the two strains having approximately equivalent c.v. at full induction.

To evaluate model predictions, we pre-grew mutant and wild-type cells in 2% raffinose and transferred them to medium containing 0.1%, 0.2%, 0.5% and 2% galactose. The fluorescence c.v. values for responding cells of the two strains at these concentrations are shown in **Figure 4b** (excluding non-responding mutant cells gives the most conservative possible c.v. measurement (see Methods)). The mutant results show the expected trend of decreasing c.v. with increasing galactose; this trend is less pronounced in wild-type cells, probably owing to negative feedback reducing noise at low induction levels. In addition, the level of the reporter in the mutant was clearly more variable than in the wild-type at each concentration tested experimentally. We experimentally measured fluorescence intensity for mutant and wild-type cells at 0.1% and 0.2% galactose (see histograms in **Fig. 4d,f**) and performed the corresponding stochastic simulations (**Fig. 4c,e**). The ratio of the mutant fluorescence c.v. to the wild-type fluorescence c.v. was consistent between the model and experimental data.

To quantify the significance of the observed 28% (± 6%) greater variability of mutant fluorescence over wild-type fluorescence after 6 h of growth on galactose, we performed four replicate experiments at 0.1% and 0.2% galactose. The null hypothesis that the mutant and wild-type steady-state c.v. measurements come from the same distribution is rejected at $P = 0.0027$ for 0.1% galactose and $P = 0.0049$ for 0.2% galactose (see Methods).

We tested experimentally the model prediction that at steady-state the mutant reporter fluorescence is consistently higher than wild-type (40% higher at 0.05% galactose and 10% higher at 2% galactose) (**Supplementary Fig. 4** and **Supplementary Table 1**). The ratio of mutant to wild-type fluorescence is 1.28 ± 0.07 averaged across galactose concentrations; the corresponding ratio from the model is 1.27.

To estimate the extent to which the delay of the *GAL* response in the mutant puts it at a potential growth disadvantage, we simulated growth of the two strains using the time-course data (see Methods), assuming a perpetually alternating raffinose-galactose medium. The results indicate that the wild-type would grow ~20% faster than the mutant (**Supplementary Fig. 5**).

We also used the model to simulate the effects of disabling the *GAL3* and *GAL80* feedback loops separately using the *CYC1* promoter (**Fig. 5**). In the case of the *GAL80* 'loop knockout', the *GAL* switch is fully induced at concentrations above 0.1% galactose. In the *GAL3* loop knockout, the *GAL* response is severely attenuated, and the overall range of *GAL* response is reduced fivefold.

We investigated how the *GAL3* (positive) and *GAL80* (negative) feedback loops in the yeast galactose use pathway control the network response to galactose. The results demonstrate two key roles of the dual-feedback architecture: (i) reducing population heterogeneity of *GAL* gene expression and (ii) enabling a rapid response.

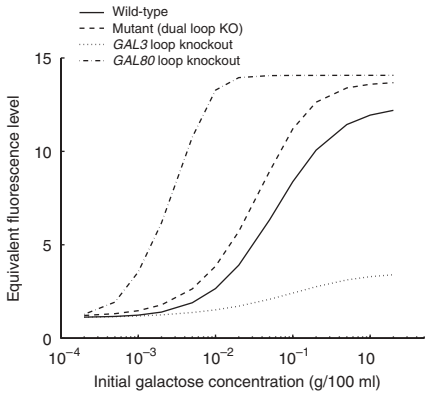

Figure 5 Simulation results showing the steady-state dose-response of four strains: wild-type, mutant (both *GAL3* and *GAL80* feedback loops disabled), *GAL3* feedback loop disabled and *GAL80* feedback loop disabled. The predicted fluorescence intensity of the *GAL1:GFP* reporter (relative to the autofluorescence of the control strain, as described in Methods) is plotted over a range of initial galactose concentrations specified in the model. The galactose response of the *GAL3* loop knockout is seen to be attenuated by approximately 80% so that the *GAL* switch is only 18% induced at 2% galactose. The *GAL80* loop knockout is seen to be hypersensitive to galactose, reaching full induction at 0.01% galactose (at which concentration the wild-type is approximately 13% induced). The inflection point of the (log) galactose dose-response in the *GAL80* loop knockout strain occurs at approximately 0.002% galactose, compared with 0.03% for the dual-loop knockout strain and 0.07% for the wild-type strain.

Simulations suggest that negative feedback through the inhibitor Gal80p is largely responsible for reducing the heterogeneity of *GAL* gene expression[19]. This is consistent with the expectation that negative feedback suppresses noise[6,7]. However, regulation of *GAL80* alone is not sufficient to ensure a functional *GAL* switch: *GAL3* must also be regulated. We illustrate this by modeling three cases: (i) the *GAL3* 'loop knockout', (ii) the *GAL80* 'loop knockout' and (iii) the dual-loop knockout.

In the first case, if *GAL80* is regulated but *GAL3* is held fixed, the *GAL* switch will malfunction in one of two ways. First, if *GAL3* is held fixed at a low level of expression, the *GAL* network response will be attenuated, never reaching full induction (**Fig. 5**). Second, if *GAL3* expression is held fixed at a high level, the *GAL* network response will saturate at a low galactose concentration, leading to inappropriate full induction[13]. If *GAL3* is held fixed at an intermediate expression level, the *GAL* switch will not fully induce to the level observed in the wild-type[13].

In the second case, a single-loop knockout of *GAL80* leads to increased heterogeneity of *GAL* gene expression[19]. Moreover, if *GAL80* is expressed at a minimal level, the *GAL* network response will saturate at a low galactose concentration[13] (**Fig. 5**). If *GAL80* is expressed at a high level, the *GAL* network will never fully induce[13].

In the third case (the dual-loop knockout case), the *GAL* network dose-response is comparable to wild-type (**Supplementary Fig. 4**), because the dual-loop knockout ensures a balance in *GAL3* versus *GAL80* expression[14] (**Supplementary Fig. 1**). However, in the dual-loop knockout (in which *GAL3* and *GAL80* are expressed at low levels), the *GAL* gene expression is more heterogeneous than in wild-type (**Fig. 4a**,**b**).

The higher *GAL* gene expression variability in the mutant occurs for two reasons. First, a basally expressed gene will generally have a higher c.v., and *GAL3* and *GAL80* are basally expressed in the mutant on galactose (**Supplementary Fig. 1**). Increased fluctuations in *GAL3* and *GAL80* cause increased heterogeneity in *GAL* gene expression[20]. Second, disabling the negative feedback through *GAL80* removes a mechanism for compensating for fluctuations in *GAL* gene expression. In the wild-type, a transient increase in *GAL* expression causes an increase in *GAL80*, which feeds back negatively on *GAL* expression (**Fig. 1**). In the mutant, this feedback is disabled; thus, even under noninducing conditions when *GAL80* is expressed at the same level as in the wild-type (**Supplementary Fig. 1**), *GAL* gene expression is more heterogeneous (**Supplementary Fig. 3**). This effect is more pronounced at lower galactose concentrations, where the reporter expression level is lower (**Fig. 4a**,**b**).

The average steady-state fluorescence of the mutant is consistently higher than the wild-type, which is likely to be due to the ratio of *GAL3*-to-*GAL80* expression. In noninducing conditions, the mutant *GAL3*-to-*GAL80* ratio is approximately double that of the wild-type. This is consistent with our kinetic model, in which the ratio is 1.75-fold higher in the mutant. Because the mutant *GAL3* and *GAL80* promoters are identical, these results suggest that the endogenous *GAL80* promoter has a higher activity than the *GAL3* promoter.

In addition to having higher *GAL* expression variability at steady state, the mutant is both delayed and more variable in its initial response to galactose. The transiently bimodal mutant response is due to two combined effects: first, the heterogeneous expression of Gal80p leads to a highly variable initial rate of induction, where cells with high Gal80p are delayed in their response; second, because *GAL80* is not being concomitantly upregulated, those mutant cells that respond after the initial delay, actually induce more rapidly (**Supplementary Fig. 2**), leaving few cells at intermediate fluorescence. The transiently bimodal response in the mutant may confer a selective disadvantage in using transiently available or low-concentration galactose (**Supplementary Fig. 5**).

The systems biology approach in this study demonstrates that the dual-feedback loops in the *GAL* regulatory network act in concert to ensure uniform induction, both dynamically and at a steady state.

METHODS

Yeast strain preparation. We modified *GAL3* and *GAL80* as follows: *URA3* was fused upstream of the minimal cytochrome-c isoform 1 (*CYC1*) promoter, comprising nucleotides –138 to –1 (where +1 is the A of the *CYC1* start codon), by sequential PCR with flanking oligomers containing ~60-bp arms homologous to either *GAL3* or *GAL80* and integrated into BY4742 or BY4741 (ref. 21), replacing nucleotides –1 to –899 of *GAL3* or nucleotides –1 to –249 of *GAL80*, respectively (see **Supplementary Table 2** for the primer sequences). *CYC1:GAL3* and *CYC1:GAL80* strains were crossed and diploids sporulated to obtain haploid strains containing both modifications. All experiments were performed using haploid yeast.

We generated the reporter gene encoding GFP+ under the control of the *GAL1* promoter by PCR (see **Supplementary Table 2** for the primer sequences). To do this, we amplified the gene encoding GFP+ (followed by *Schizosaccharomyces pombe HIS5*) from pGFP+/*HIS5* by replacing EGFP in pGFP/*HIS5* (ref. 22) with GFP+ (ref. 23). We amplified the *GAL1* promoter, consisting of nucleotides –12 to –690, from genomic DNA; we fused the two PCR products by PCR using flanking oligomers containing ~60-bp sequences homologous to *HIS3*. The gene fusion was integrated into BY4741 and into an isogenic strain containing both *GAL3* and *GAL80* modifications, replacing +1 to +400 of the *his3*Δ1 locus. Strains with galactose-dependent green fluorescence were selected by fluorescence microscopy.

All strains used (see above) were *MEL1*-deficient. Their inability to break down melibiose into galactose + glucose[24] was confirmed by observing the equivalent autofluorescence (within the experimental uncertainty) of the wild-type strain and a control strain grown on raffinose (**Supplementary Figure 1**). The background strain (without the GFP reporter construct) was used as the control strain for flow cytofluorometry. The minimal *CYC1* promoter has been

shown to cause basal expression that is insensitive to the extracellular galactose concentration[25]. The *GAL1* promoter driving the reporter gene contains all four Gal4p binding sites[10].

Model details. The complete description of the model is presented in the **Supplementary Note** (see also an earlier version in refs. 19,20); here we provide a brief overview. The *GAL* model used in this study contains 44 unidirectional biochemical reactions through which 19 species interact. The species include proteins and mRNAs for the genes *GAL1*, *GAL2*, *GAL80*, *GAL3*, *GAL1:GFP* (the reporter gene) and intracellular galactose (GAI). The dimer and monomer forms of Gal3p and Gal80p are modeled, as well as the shuttling of Gal80p between the nucleus and cytoplasm[14]. The steps of the metabolic pathway that are modeled include only galactose transport into the cell and the conversion of galactose to galactose-1-phosphate by the galactokinase Gal1p. Protein-DNA interactions are assumed to occur sufficiently rapidly that binding and releasing reactions from DNA are assumed to be at quasi–steady-state (QSS)[26] with respect to the free transcription factor concentration in the nucleus. This allows the use of a continuous fractional activation function in place of modeling individual protein-DNA binding events[27]. The equilibrium dissociation constants for Gal3p activation given in ref. 13 and the fractional activation levels for a single Gal4p binding site given in ref. 14 were used in the model. The equilibrium dissociation constant for Gal3p*-Gal80p (Gal3p* denotes activated Gal3p) complex formation was the remaining important free parameter in the model; it was adjusted to give a fractional activity for the reporter gene (**Supplementary Fig. 4**) consistent with the experimentally measured activity in 0.1% galactose.

The mutant strain was modeled by substituting a fixed fractional activity f_{mut} for the *GAL3* and *GAL80* genes comparable to the basal expression of these genes in the wild-type on raffinose[19]. The values of f_{mut} in the range 0.04–0.06 were found to be consistent with the steady-state coefficient of variation data (**Fig. 4a**). The model assumes a constant extracellular concentration of galactose, corresponding to a continuous culture system. The following numbers of Gal4p binding sites were assumed for the different *GAL* promoters: one binding site for *GAL3* and *GAL80*; five binding sites for *GAL2* and four binding sites for *GAL1*[10].

Simulations. All simulations of the *GAL* model were performed using the Dizzy software program[27]. The dynamics of the model were solved in two steps. (i) The steady-state was obtained by numerically solving (to 2,000 min) the deterministic kinetics as a system of ordinary differential equations (ODEs). The steady-state results were used as the initial conditions for the stochastic simulations. (ii) The stochastic dynamics were solved using a Monte Carlo technique in which the results were averaged over an ensemble of realizations of a Markov process representing the stochastic kinetics (see **Supplementary Note** for details). The initial conditions for the time course simulations for the mutant strain were modified to double the amount of Gal80p, in order to model the delay observed in the mutant strain induction; this did not affect the steady-state predictions of the model. We obtained the histogram of reporter molecule concentrations from the stochastic simulations and compared it with the histogram of the relative fluorescence intensity from the flow cytometry data.

The QSS model was obtained by solving the algebraic steady-state equations for the kinetic model, assuming that all equations are at quasi–steady-state with respect to the slowly time-varying internal galactose (GAI) concentration[13]. The equations were simplified analytically and then solved numerically using Mathematica (Wolfram). The QSS model agrees with the solution of the full ODE model at steady state.

We obtained the growth curves in **Supplementary Figure 5** using an ordinary differential equation (ODE) model in which each strain has a time-dependent specific growth rate. In raffinose, the specific growth rate is ln(2) divided by the average division time of 6 h (J.D.A., unpublished). In galactose, the time-dependent specific growth rate is given by the fraction of responding cells, as shown in **Figure 2b**, divided by the division time of 3 h. The growth equations were solved using Mathematica.

Flow cytometry. All yeast strains were grown overnight in YEP (1% yeast extract, 2% peptone) with 2% glucose (YEPD) (all wt/vol), washed and transferred to YEP containing 2% raffinose (YEPR) and grown for 16 h at 30 °C. Cells were collected and induced in YEPR or YEP supplemented with galactose (YEPG) at the concentrations indicated for the amount of time indicated in the text (0–7 h for the time-course experiments, 6 h for the dose-response experiments). Induced cells were suspended at 1×10^6 to 10×10^6 cells/ml in the induction medium and were measured on a high-speed inFlux cell sorter (Cytopeia). Cells were analyzed based on scattered laser light and fluorescence from a focused 488-nm argon ion laser operating at 300 mW. The data for each event consisted of an ordered tuple of the forward light scatter (FSC), perpendicular light scatter (SSC), pulse width of the forward scattered light and the integrated fluorescence from 510–550 nm to quantify the GFP concentration. Data from a single run of the flow cytometer were stored in a Flow Cytometry Standard (FCS) v.3.0 format file incorporating 50,000 events. Initial visualization of the flow cytometry data was performed using Summit Offline (DakoCytomation) v.3.1. A negative control strain (wild-type, without the GFP reporter) was cultured in 2% raffinose for 16 h and analyzed using flow cytometry to obtain basal autofluorescence data. Fluorescence measurements of all events were normalized relative to the median fluorescence of the control strain from the corresponding replicate experiment. The increase in the c.v. in the mutant strain shown in **Figure 4b** is a galactose effect: the strains are similar in size (**Supplementary Note**) and there is no measurable c.v. difference in noninducing conditions (**Supplementary Fig. 1**).

Quantitative PCR (Q-PCR). We used Q-PCR to establish the relative mRNA levels of *GAL80* and *GAL3* in the wild-type and mutant strains (as defined in 'Yeast strain preparation' section of Methods). Cells were grown in 2% raffinose or 0.1% galactose for 6 h as described in 'Flow cytometry' section of Methods and total RNA was isolated using hot acid phenol extraction. cDNA was prepared using TaqMan reverse transcription reagents with random primers (Applied Biosystems). We performed Q-PCR using a 7900 HT Fast Real-time PCR system and Power SYBR(r) Green PCR Master Mix (Applied Biosystems) in duplicate using two different primer pairs for each gene (see **Supplementary Table 2** for the primer sequences). Expression units in **Supplementary Figure 1** were computed relative to the expression level of *NUP170*, which has stable expression that is insensitive to galactose[28].

Data analysis. The flow cytometry data were converted to a text file format using Bioconductor (http://www.bioconductor.org) and then analyzed using Matlab (Mathworks). For each data point, we computed the ratio of the forward light scatter (FLS) to the average FLS of the control strain as well as the ratio of the fluorescence intensity (FLI) to the average FLI of the control strain. To select events with homogeneous cell size and avoid fluorescence variation coming from cell size variation, we selected events within a narrow window of FLS based on the mean FLS $\pm$ 0.1 $\times$ s.d. of the FLS of the control strain. Mutant and wild-type data were gated with the same FLS window size to avoid introducing bias. For calculating the c.v. of induced cells, only those cells with a fluorescence greater than three times the autofluorescence of the control strain ('responding' cells) were included. At this value for the cutoff, $\sim$0% of cells were responding, for either strain, on 2% raffinose. Computing the c.v. using only the responding cells eliminates variability in the mutant strain originating from the weakly bimodal distribution at 6 h and is therefore a conservative method of computing the cellular heterogeneity. To calibrate the number of reporter molecules in the model with observed fluorescence intensity, we used the function $F = 1 + R/C$, where R is the number of reporter molecules predicted for the strain and condition, F is the observed fluorescence ratio (relative to the control strain autofluorescence) and C is a scale parameter[29]. The scale parameter was obtained by a least-squares fit of the time course predictions from the kinetic model to the experimentally measured time course fluorescence values, with the above formula. The parameter value used throughout the study was $C = 1{,}262.2$. The actual number of GFP molecules *in vivo* was not measured, so the constant C can be used only for converting between the model and the fluorescence data.

Statistical analysis. We tested the null hypothesis that the replicate-averaged c.v. values of the mutant and wild-type fluorescence come from the same distribution using a two-tailed *t*-test in Matlab (Mathworks) to obtain a *P* value. (The *P* value is the probability of observing (by chance) the given deviations (between mutant and wild-type) of the average c.v., assuming the

null hypothesis; it is related to the confidence C by $P = 1 - C$.) Separate tests were performed for the 0.1% and 0.2% galactose cases. Four replicates were conducted per strain (and condition); thus, each test had a combined six degrees of freedom. The test was performed without assuming equal variances of the two data sets.

Note: Supplementary information is available on the Nature Genetics website.

ACKNOWLEDGMENTS

We thank D. Hwang for helpful advice on the statistical analysis, H. Kostner for assistance with the QPCR experiments and E. Schweighofer for assistance with the cluster computing infrastructure. This work was supported in part by grants from the US National Institutes of Health (GM076547, GM067228).

AUTHOR CONTRIBUTIONS

S.A.R., J.J.S., D.O., H.B. and J.D.A. designed the study. J.J.S., M.M. and T.W.P. carried out the experimental validation. S.A.R., D.O. and P.A. performed the modeling and simulations. S.A.R., J.J.S., H.B. and J.D.A. wrote the paper.

COMPETING INTERESTS STATEMENT

The authors declare that they have no competing financial interests.

Published online at http://www.nature.com/naturegenetics
Reprints and permissions information is available online at http://npg.nature.com/reprintsandpermissions/

1. Blake, W.J., Kærn, M., Cantor, C.R. & Collins, J.J. Noise in eukaryotic gene expression. *Nature* **422**, 633–637 (2003).
2. Kærn, M., Elston, T.C., Blake, W.J. & Collins, J.J. Stochasticity in gene expression: from theories to phenotypes. *Nat. Rev. Genet.* **6**, 451–464 (2005).
3. Ozbudak, E.M., Thattai, M., Kurtser, I., Grossman, A.D. & van Oudenaarden, A. Regulation of noise in the expression of a single gene. *Nat. Genet.* **31**, 69–73 (2002).
4. Raser, J.M. & O'Shea, E.K. Control of stochasticity in eukaryotic gene expression. *Science* **304**, 1811–1814 (2004).
5. Volfson, D. *et al.* Origins of extrinsic variability in eukaryotic gene expression. *Nature* **439**, 861–864 (2006).
6. Becskei, A. & Serrano, L. Engineering stability in gene networks by autoregulation. *Nature* **405**, 590–593 (2000).
7. Orrell, D. & Bolouri, H. Control of internal and external noise in genetic regulatory networks. *J. Theor. Biol.* **230**, 301–312 (2004).
8. Brandman, O., Ferrell, J.E., Jr., Li, R. & Meyer, T. Interlinked fast and slow positive feedback loops drive reliable cell decisions. *Science* **310**, 496–498 (2005).
9. Hasty, J., Pradines, J., Dolnik, M. & Collins, J.J. Noise-based switches and amplifiers for gene expression. *Proc. Natl. Acad. Sci. USA* **97**, 2075–2080 (2000).
10. Melcher, K. Galactose metabolism in *Saccharomyces cerevisiae*: a paradigm for eukaryotic gene regulation. in *Yeast Sugar Metabolism* (eds. Zimmermann, F.K. & Entian, K.-D.) (North Holland, Lancaster, Pennsylvania, 1997).
11. Peng, G. & Hopper, J.E. Gene activation by interaction of an inhibitor with a cytoplasmic signaling protein. *Proc. Natl. Acad. Sci. USA* **99**, 8548–8553 (2002).
12. Platt, A. & Reece, R.J. The yeast galactose genetic switch is mediated by the formation of Gal4p-Gal80p-Gal3p complex. *EMBO J.* **17**, 4086–4091 (1998).
13. Acar, M., Becskei, A. & van Oudenaarden, A. Enhancement of cellular memory by reducing stochastic transitions. *Nature* **435**, 228–232 (2005).
14. Verma, M., Bhat, P.J. & Venkatesh, K.V. Quantitative analysis of *GAL* genetic switch of *Saccharomyces cerevisiae* reveals that nuclearcytoplasmic shuttling of Gal80p results in a highly sensitive response to galactose. *J. Biol. Chem.* **278**, 48764–48769 (2003).
15. Ruhela, A. *et al.* Autoregulation of regulatory proteins is key for dynamic operation of *GAL* switch in *Saccharomyces cerevisiae*. *FEBS Lett.* **576**, 119–126 (2004).
16. Biggar, S.R. & Crabtree, G.R. Cell signaling can direct either binary or graded transcriptional responses. *EMBO J.* **20**, 3167–3176 (2001).
17. Verma, M., Bhat, P.J., Bhartiya, S. & Venkatesh, K.V. A steady-state modeling approach to validate an *in vivo* mechanism of the *GAL* regulatory network in *Saccharomyces cerevisiae*. *Eur. J. Biochem.* **271**, 4064–4074 (2004).
18. Rosenfeld, N., Elowitz, M.B. & Alon, U. Negative autoregulation speeds the response times of transcriptional networks. *J. Mol. Biol.* **323**, 785–793 (2002).
19. de Atauri, P., Orrell, D., Ramsey, S. & Bolouri, H. Evolution of 'design' principles in biochemical networks. *IEE Proc. Sys. Biol.* **1**, 28–40 (2004).
20. Orrell, D. *et al.* Feedback control of stochastic noise in the yeast galactose utilization pathway. *Physica D.* **217**, 64–76 (2006).
21. Brachmann, C.B. *et al.* Designer deletion strains derived from *Saccharomyces cerevisiae* S288C: a useful set of strains and plasmids for PCR-mediated gene disruption and other applications preference. *Yeast* **14**, 115–132 (1998).
22. Dilworth, D.J. *et al.* Nup2p dynamically associates with the distal regions of the yeast nuclear pore complex. *J. Cell Biol.* **153**, 1465–1478 (2001).
23. Scholz, O., Thiel, A., Hillen, W. & Niederweis, M. Quantitative analysis of gene expression with an improved green fluorescent protein. *Eur. J. Biochem.* **267**, 1565–1570 (2000).
24. Ostergaard, S., Olsson, L. & Nielsen, J. Metabolic engineering of *Saccharomyces cerevisiae*. *Microbiol. Mol. Biol. Rev.* **64**, 34–50 (2000).
25. Guarente, L., Yocum, R.R. & Gifford, P.A. *GAL10–CYC1* hybrid yeast promoter identifies the *GAL4* regulatory region as an upstream site. *Proc. Natl. Acad. Sci. USA* **79**, 7410–7414 (1982).
26. Rao, C.V. & Arkin, A.P. Stochastic chemical kinetics and the quasi-steady-state assumption: Application to the Gillespie algorithm. *J. Chem. Phys.* **118**, 4999–5010 (2003).
27. Ramsey, S., Orrell, D. & Bolouri, H. Dizzy: Stochastic simulations of large-scale genetic regulatory networks. *J. Bioinform. Comput. Biol.* **3**, 437–454 (2005).
28. Gasch, A.P. *et al.* Genomic expression programs in the response of yeast cells to environmental changes. *Mol. Biol. Cell* **11**, 4241–4257 (2000).
29. Pédelacq, J.-D., Cabantous, S., Tran, T., Terwilliger, T.C. & Waldo, G.S. Engineering and characterization of a superfolder green fluorescent protein. *Nature Biotech.* **24**, 79–88 (2006).
30. Lue, N.F., Chasman, D.I., Buchman, A.R. & Kornberg, R.D. Interaction of *GAL4* and *GAL80* gene regulatory proteins *in vitro*. *Mol. Cell. Biol.* **7**, 3446–3451 (1987).